Improved reliability in parameter estimation of dynamic nonlinear systems with sparse data incorporating a priori information

van Boxtel, S.

Award date:
2006

Eindhoven University of Technology
Department of Electrical Engineering
Control Systems

TU/e technische universiteit eindhoven

Improved reliability in parameter estimation of dynamic nonlinear systems with sparse data incorporating a priori information

by

S. van Boxtel

Master of Science thesis

Project period: May 2006
Report Number: 06A/07
Commissioned by: Prof.Dr.Ir. P.P.J. van den Bosch

Supervisor: Dr.Ir. N.A.W. van Riel

Improved reliability in parameter estimation of dynamic nonlinear systems with sparse data incorporating a priori information

A myocardial calcium handling case study

Sander van Boxtel

Abstract

This study deals with a new method to improve the reliability of parameter estimates in system identification of dynamic nonlinear systems that suffer from sparse data. This technique consists of incorporating a priori information from available secondary information sources concerning system variables into the minimization algorithm. Additional 'data' is derived from this a priori information and used together with the sparse experimental data in a weighted objective optimization. As a representative example of a dynamic nonlinear system with sparse data, the calcium handling of in vivo rat myocardia is used as a case study, where the four model parameter estimates are highly unreliable when only experimental data is used for system identification. This reliability is relevant because in biomedical research there is an increasing need to study intact systems, in contrast to in vitro research. The results show an increased reliability of the estimated parameters. This reliability is measured with use of properties from the Fisher information matrix. This study shows that incorporating a priori information concerning system variables is a flexible approach when dealing with sparse data, improving the reliability of model parameter estimates.

1 Introduction

Parameter estimation and system identification are more and more common applied technologies in a wide variety of research disciplines nowadays. Based on experimental data and observations dynamical nonlinear systems are described in mathematical models. These models give insight in the behavior of the system. In clinical physiology models are used for classification of important system conditions (e.g. concerning health), where different values of the estimated in vivo model parameters indicate the different conditions. Also the effects of for example medical treatments can be evaluated when looking at these model parameters [Buijs, 2005].

In contrast to, for example, electrical and mechanical systems, where (electrical) signals can be measured relatively easy at various points in the system, biomedical systems have often only a few observations. Due to ethical, technological, but also financial limitations often not all the system's variables and

conditions can be measured, covering merely a limited part of the total system's dynamics. The lack of sufficient experimental measurements makes it difficult to properly identify a system, and estimate model parameters with sufficient accuracy. Despite these limitations accurate parameter estimates are of high importance when classification depends on it. For this, new techniques have to be considered.

Besides using experimental data for system identification, possibly other data is available from literature, that can be used as an alternative source of information for system identification. This so called a priori information originates from conclusions of former research about the actual behavior of (separate parts of) the system. If this a priori information is present, it can be used as extra 'datapoints', in addition to the experimental data in a combined objective function. This function will be used in the numerical optimization problem that has to be solved to estimate the model parameters.

This study deals with the incorporation of additional a priori information in the system identification. The goal is to investigate if and how the identifiability of the system and the reliability of the estimated parameters can be improved. When normal identification techniques fail due to the scarcity of experimental data, it will be shown that the techniques presented in this study can cope with this deficiency.

The presented techniques were applied to the system identification of calcium handling in the myocardium of an intact rat heart. Calcium is the main regulator of the contraction and relaxation of the heart's ventricles. The study of the calcium transients in the myocardium involves the study of the Sarcoplasmic Reticulum Ca^{2+}-ATPase (SERCA), which is known as the most important calcium extrusion pump. A three compartment model was proposed, and the calcium concentration $[Ca^{2+}]$ of only one compartment is available as experimental time-series data. This concentration is measured by illuminating an isolated ex vivo beating rat heart in which a fluorescent dye is loaded. A non-linear differential equation is proposed with four unknown modelparameters. Important a priori information is obtained from beat to beat flux ratios between the compartments.

The outline of this article is as follows; First, this article explains how the experimental data and a priori information is combined in one optimization criterion (section 2). Also the methods to evaluate the model parameter estimates are presented in this section. Section 3 presents the case study, where a model of the calcium handling in the myocardium is proposed, and an additional source of information for this case is introduced. To further improve the identifiability of SERCA, changes in the experiment design were proposed, which is presented in section 4. The results are presented in section 5, and this article ends with a discussion to evaluate the presented methods and results (section 6), and the final conclusions (section 7). Additional information concerning figures and tables, and derivations of equations, as well as the implemented source code, can be found in the appendices.

2 Methods

Weighted objective optimization

A nonlinear dynamic system with states $\boldsymbol{x}$, input $\boldsymbol{u}$, output $\hat{\boldsymbol{y}}$ and model parameters $\boldsymbol{\theta}$ is generally described as follows;

$$\begin{aligned} \dot{\boldsymbol{x}}(t,\boldsymbol{\theta}) &= f(\boldsymbol{x}(t,\boldsymbol{\theta}),\boldsymbol{u}(t),\boldsymbol{\theta}) \\ \hat{\boldsymbol{y}}(t,\boldsymbol{\theta}) &= g(\boldsymbol{x}(t,\boldsymbol{\theta}),\boldsymbol{u}(t)) \end{aligned} \tag{1}$$

with initial condition $\boldsymbol{x}(0,\boldsymbol{\theta}) = \boldsymbol{x}_0$. By solving the dynamical differential equation numerically, the modeled system output $\hat{\boldsymbol{y}}(t,\hat{\boldsymbol{\theta}})$ is generated. This output can be compared to available discrete noisy experimental data $\boldsymbol{y}$ in a least squares algorithm. Assuming the system is in the model set, i.e. data does not con-

tain unmodeled dynamics, and the residual vector ξ can be characterized as white noise for $\hat{\boldsymbol{\theta}} = \boldsymbol{\theta}_{true}$, where $\hat{\boldsymbol{\theta}}$ is the estimated parameter vector and $\boldsymbol{\theta}_{true}$ is the true unknown parameter vector, the cost function $F_1(\hat{\boldsymbol{\theta}})$ can be derived from the likelihood function of a normal distribution [Damen, 2003];

$$F_1(\hat{\boldsymbol{\theta}}) = \frac{1}{2\sigma_{\xi_1}^2} \cdot \sum_{k=1}^{K} (\hat{y}_1(k, \hat{\boldsymbol{\theta}}) - y_1(k, \boldsymbol{\theta}_{true}))^2 \tag{2}$$

where $\sigma_{\xi_1}^2$ is the variance of the residuals $\xi_1(k) = \hat{y}_1(k, \hat{\boldsymbol{\theta}}) - y_1(k)$, with $\hat{y}_1(k, \hat{\boldsymbol{\theta}})$ the simulated time-series model output at sample $k = t/f_s$ (f_s is the sample frequency) with model parameters $\hat{\boldsymbol{\theta}}$ and $y_1(k, \boldsymbol{\theta}_{true})$ the experimental time-series system output at sample k. See appendix A for this derivation.

Besides experimental time-series system output, secondary sources of information can be available. This a priori information q is not necessary time-dependent, and can be assumed valid for all subjects under study. Assuming a periodic system, quite common for biomedical systems, q can be a condition that is valid every system cycle, for example. If this quantity can also be derived from the model as a periodic model output, a cost function similar to equation 2 can be derived;

$$F_2(\hat{\boldsymbol{\theta}}) = \frac{1}{2\sigma_{\xi_2}^2} \cdot \sum_{m=1}^{M} (\hat{y}_2(m, \hat{\boldsymbol{\theta}}) - q)^2 \tag{3}$$

Here, $\sigma_{\xi_2}^2$ is the variance of the residuals $\xi_2(m) = \hat{y}_2(m, \hat{\boldsymbol{\theta}}) - q$, with $\hat{y}_2(m, \hat{\boldsymbol{\theta}})$ the simulated time-series model output at sample m.

When dealing with more optimization objectives, the combination of the cost functions can guide the model parameters in specific areas of the solution space. Cost functions for the various objectives can be constructed from multiple datasets, a priori information, or potential boundary conditions on parameter values (as a penalty function).

Dimensional differences and differences in priority between the objectives suggest the use of weighting factors. This result in one combined cost function;

$$F_{tot}(\hat{\boldsymbol{\theta}}) = \sum w_i F_i(\hat{\boldsymbol{\theta}}) \tag{4}$$

Fisher information matrix

Properties of the Fisher information matrix (FIM) can be used as criteria to evaluate estimated model parameters and indicate changes in the identifiability when models are changed or experiments are redesigned. The FIM provides measures about the amount of information of a certain parameter combination, and its inverse indicates the lower bound on parameter variances.

The FIM is a positive definite, square symmetric $n \times n$ matrix (n is the number of parameters). If J is the Jacobian, defined as the $n \times D$ matrix of first derivatives of the residualvector to the parameters ($D = K + M$ is the total number of samples), the FIM for $F_{tot}(\theta)$ is constructed as follows [Flaherty, 2005];

$$\text{FIM}(\hat{\boldsymbol{\theta}}) = \frac{1}{\sigma_{\xi_{tot}}^2} \cdot J^T(\hat{\boldsymbol{\theta}}) \cdot J(\hat{\boldsymbol{\theta}}) \tag{5}$$

The minimal uncertainty, defined as the covariance matrix, is reciprocal to the FIM [Ober, 2002], and the minimal standard deviation of the estimated model parameters is calculated as the square root of this uncertainty;

$$\sigma_{\hat{\theta}_i} = \sqrt{\text{FIM}(\hat{\boldsymbol{\theta}})_{ii}^{-1}} \tag{6}$$

The positive definiteness of the FIM guarantees that all eigenvalues λ_i of the eigenvalue decomposition are positive. The eigenvectors $V = [v_1, \ldots, v_n]$ define the principal information directions in the n-dimensional parameter solution space, and the eigenvalues and

its inverse are a measure of the information, respectively uncertainty in these principal directions. This can be explained by taking an (hyper)ellipsoid and writing it in a quadratic form [Hidalgo, 2000];

$$V^T C^{-1} V = 1 \tag{7}$$

which equals the eigenvalue decomposition of FIM, with V the eigenvectors and C a diagonal matrix with the square roots of the eigenvalues λ_i on the diagonal. In a two dimensional case this approach can be graphically represented by a two dimensional ellipsoid (figure 1).

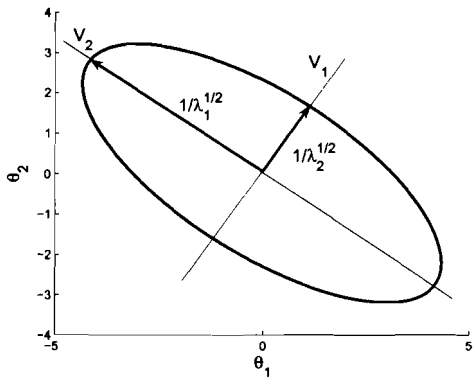

Figure 1: Graphical interpretation of two-dimensional FIM. This ellips shows the amount of information for a certain estimated parameter combination. The length and phase of the axes are determined by the eigenvalues and eigenvectors of the FIM.

Model-to-model identification

System identification deals with the comparison of simulated model output and real experimental system output. The goal of this so called model-to-data identification is the estimation of the model parameters.

To get a first glance at the possible problem areas and identifiability issues of the system, the model can be presented also as a real 'system', only this time with a known set of model parameters $\boldsymbol{\theta}_{true}$. This 'system' is in the modelset, and when no noise is added, the global minimum is known (namely, for $\boldsymbol{\theta} = \boldsymbol{\theta}_{true}$). This model-to-model identification can be used for example to draw two dimensional contourplots for θ_i and θ_j $(i \neq j)$ with the other parameters fixed, to show the surroundings of the global minimum, which can be very useful to show potential deviations and biasses on the model parameters. This will be shown in section 5.

Implementation

All numerical methods where implemented in Matlab 7.04 (R14) using a personal computer with Windows XP Pro running on an Intel Pentium 4 processor with 2.69 GHz and 1 Gb of RAM. For solving the model's differential equation a variable step ODE-solver (ode23) was used, with predefined maximal step size to assure proper step sizes. For the parameter estimation the optimization toolbox was used, where a Trust region method was selected (lsqnonlin). With this method it was possible to select parameter boundaries, and a lower bound at zero was chosen for all modelparameters. Other available algorithms were Gauss-Newton and Levenberg Marquardt, but were less favorable here, because their lack of boundary options.

3 Case study: calcium handling in myocardium

In this section an example is presented of a dynamic nonlinear biomedical system that suffers from sparse data. The above described technique of weighted objective optimization is used on this case, and properties of the FIM are used to evaluate the results.

The case deals with the calcium handling of an intact rat myocardium. In this section, the model is presented, and the available a priori information is explained. Further, the result section shows the results of the research on

the case study.

Myocardium model

The working of the heart, with the contraction and relaxation of the heart's ventricles as most important function, is caused mainly by the calcium transients through the various organelles of the muscle fibers. The dynamics of the calcium transients have been modeled by a three compartment model, consisting of the extracellular space (perfused with Krebs-Henseleit solution) with calcium concentration $[Ca^{2+}]_{ex}$ ($[M]$), the sarcoplasm reticulum (SR) with calcium concentration $[Ca^{2+}]_{sr}$ ($[M]$) and the sarcoplasm with the intracellular free calcium concentration $[Ca^{2+}]_i$ ($[M]$). Figure 2 shows a schematic overview of this model with the major in- and effluxes. The sarcoplasm is the compartment of interest, because here the calcium stimulates the contractile proteins, responsible for the contraction. The following nonlinear dynamic model of the sarcoplasm was proposed
[Riel, 2003];

$$\begin{aligned} \dot{x} &= \frac{I_{in}(x)\cdot u(t) - I_{eff}(x)}{B(x)} \\ y_1 &= x \end{aligned} \tag{8}$$

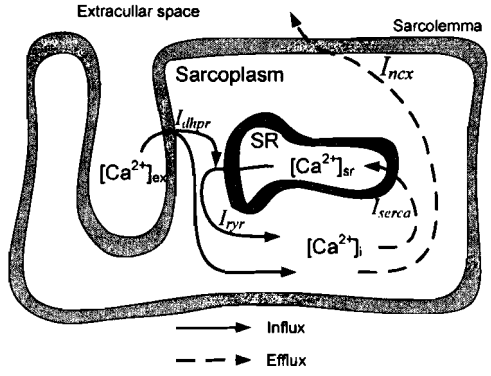

Figure 2: Schematic overview of calcium flows through myocardium. The three compartments are visible (Extracellular space, SR and sarcoplasm), and also the major in- and effluxes.

The output y_1 is the free intracellular calcium concentration $[Ca^{2+}]_i$, $I_{in} = I_{dhpr} + I_{ryr}$ ($[M/s]$) is the total inflow in the sarcoplasm and $I_{eff} = I_{ncx} + I_{serca}$ ($[M/s]$) the total efflux. The differential equation includes all major calcium fluxes between the sarcoplasm and other two compartments. I_{dhpr} and I_{ryr} represent the inflow through the sarcolemma (SL) (by dihydropyridine receptors) and SR membrane (by ryanodine receptors), respectively. Both are activated by an input u, which is a trigger signal resembling the action potential. The Na^+/Ca^{2+} exchanger (NCX) and SERCA are the two most important pumps (I_{ncx} and I_{serca}), causing the free intracellular calcium concentration $[Ca^{2+}]_i$ to flow out of the cytoplasm to a steady state level. In addition to the fluxes, calcium homeostasis is attained with the presence of various calcium buffers, represented in B ([-]). This buffering has been described by the rapid buffer approximation [Wagner, 1994];

$$B = 1 + \sum \frac{[B_i]k_i}{(k_i + [Ca^{2+}]_i)^2} \tag{9}$$

with $[B]_i$ ($[M]$) the concentration and k_i ($[M]$) the dissociation constants of calcium buffer i. An overview of these values can be found in literature [Balke, 1994].

I_{ncx} and I_{serca} both depend on the total free calcium concentration in the cytoplasm. For modeling I_{serca} a Hill equation was proposed [Lytton, 1992], with a saturation flow V_m ($[M/s]$), affinity coefficient k_m ($[M]$) and a Hill coefficient of 2.

$$I_{serca} = V_m \cdot \frac{[Ca^{2+}]_i^2}{[Ca^{2+}]_i^2 + k_m^2} \tag{10}$$

In the physiological range NCX is modeled as a linear function of the cytoplasmic calcium concentration
[Hove-Madsen, 2001];

$$I_{ncx} = k_{ncx} \cdot [Ca^{2+}]_i \tag{11}$$

with k_{ncx} ($[s^{-1}]$) the rate coefficient. The separate influx mechanisms I_{dhpr} and I_{ryr} are dependent of respectively the SL and SR mem-

brane permeability and the calcium concentration gradient (Fick's Law of Diffusion);

$$I_r = g_r \cdot ([Ca^{2+}]_c - [Ca^{2+}]_i)$$
$$r = \{dhpr, ryr\} \quad (12)$$
$$c = \{extracellular\ space, SR\}$$

Here g_r ($[s^{-1}]$) is the permeability of respectively the SL and SR membrane, and $[Ca^{2+}]_c$ ($[M]$) respectively the calcium concentration in the extracellular space and the SR. I_{ryr} is initiated by I_{dhpr}, which is called the calcium-induced calcium-release (CICR) mechanism [Fabiato, 1983]. The time between inducing and releasing is very small compared to the total systolic time, and the CICR is therefor omitted. Both channels can therefor be combined, with a lumped permeability g_l ($[s^{-1}]$);

$$I_{in} = g_l \cdot mean([Ca^{2+}]_{ex}, [Ca^{2+}]_{sr}) \quad (13)$$

$[Ca^{2+}]_i$ is neglected here, because both the extracellular and SR concentration ($\sim mM$) are much bigger than the sarcoplasmic concentration ($\sim \mu M$). The extracellular calcium concentration $[Ca^{2+}]_{ex}$ was experimentally set at a constant value $[Ca^{2+}]_{ex0}$ (1.5mM) [Riel, 2003], and due to several buffering proteins, the SR calcium concentration $[Ca^{2+}]_{sr}$ is kept nearly constant at $[Ca^{2+}]_{sr0}$ under normal conditions [Bers, 2002]. The action potential $u(t)$ ([-]) is the electrical activity that stimulates the sarcolemmal membrane (and indirectly the SR membrane) to let calcium through into the cytoplasm. This action potential can be described as a 4^{th}-order Sigmoid function, dependent of cardiac cycle time, with t_h ($[s]$) the moment the maximal influx is halfway [Buijs, 2005].

$$u(t) = 1 - \frac{t^4}{t^4 + t_h^4} \quad 0 < t \leq T \quad (14)$$

The halftime t_h can be approximated as the moment the maximal total cytoplasmic flux is halfway. Above equations result in four unknown modelparameters, listed in table 1.

Table 1: The four model parameters with their physiological meaning and unity.

Par.	Description	Unity
V_m	Max. SERCA flow	Ms^{-1}
k_m	Affinity coeff. SERCA	M
k_{ncx}	Rate coeff. NCX	s^{-1}
g_l	Permeability of SL/SR	s^{-1}

A priori information

Bers [Bers, 2002] states that the removal of calcium from the sarcoplasm is achieved by several routes. In rat myocardia 92% of the total free calcium concentration is removed by the SERCA, and the remaining 8% by NCX and other slow systems. This quantative information is originating from estimates done in [Bassani, 1994].

Besides the time-series data of intracellular calcium concentrations, which is measured directly from one heart, the efflux-ratio is a priori information q, assumed to be valid independent of time and subject. To use this information in the optimization procedure, the simulated efflux-ratio has to be calculated for each heart beat. The calcium concentration that flows out through a pump with a flow $I(t)$ during a time t_f equals the integral of the flow over a time period t_f.

$$\Delta[Ca^{2+}](i \rightarrow c) = \int^{t_f} I_C \, dt \quad (15)$$

Here, c = {extracellular space, SR} are the different compartments the calcium flows out to and C = {ncx, serca} are the two pumps responsible for the calcium transport. A secondary model output $\hat{y}_2(m, \hat{\boldsymbol{\theta}})$ then looks as follows;

$$\hat{y}_2(m, \hat{\boldsymbol{\theta}}) = \frac{\int_{mT-t_f}^{mT} I_{serca} \, dt}{\int_{mT-t_f}^{mT} I_{ncx} \, dt} \quad (16)$$

The only a priori information concerning the model parameters directly is the non negativeness of the parameters. Because the parameters all represent a physiological quantity which can not become negative, all four model parameters have a lower bound of zero. A physiological upper bound also exist, but no information is available about this maximum, so the model parameters are limited to the range $[0, \infty]$.

4 Optimal experiment design

Section 3 presented a kinetic model of SERCA (equation 10), with a maximal calciumflux V_m and affinity coefficient k_m as the unknown model parameters. Estimating these kinetic parameters is a difficult task, due to the low identifiability of the pump. Given normal conditions, this system was shown not to be identifiable, and estimates were very unreliable (see the final results in section 5). Figure 3 shows the modeled kinetics of SERCA for a simulated control situation, i.e. without perturbation.

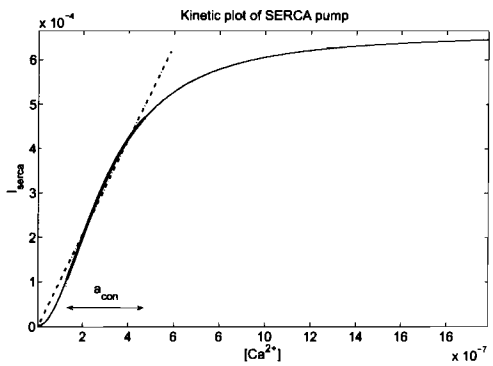

Figure 3: Modeled SERCA kinetics of control experiment. The Hill equation (solid) was proposed in section 3. Based on the experimental range (indicated by a_{con}) also a linear model can be proposed (dash-dot).

a_{con} is the range of the experimental calcium transients as the difference between end-systolic and end-diastolic concentrations. To reveal the complete kinetics of SERCA, this range is not sufficient, as can be seen in the plot. Given the small range of calcium concentrations, a linear model seems appropriate, where only one parameter is needed. The fact that two parameters are used for modeling SERCA can be seen as an overcompensation, resulting in the low identifiability. Changes in the experiment design can result in higher transients, expected to overcome this problem. With a bigger concentration range, the linear relationship will not suffice, and the model based on the two parameter Hill equation will be better identifiable.

A larger amplitude is reached when Isoproterenol is perfused in the myocardium. Isoproterenol is a well known β-adrenergic stimulator, increasing contractility of the muscle fibers, caused by larger calcium transients [Ruijs, 2006]. Looking at figure 3, it is expected that a bigger amplitude will improve the identifiability of SERCA.

Besides higher calcium concentrations, isoproterenol also effects the heart rate. Figure 4 shows a power spectral density plot of the calcium transients of a control and stimulated rat myocardium, showing the main differences in amplitude and the smaller difference in frequency. Eventually, a double effect occurs. Besides an increased calcium concentration due to a change of SERCA, also the higher heartrate (pacing) helps increasing the end-diastolic concentration [Ruijs, 2006].

Caution has to be taken with the calcium concentration in the SR. An increased working of SERCA results in an increased influx from the SR to the cytoplasm, due to a larger concentration gradient (equation 12). This larger concentration gradient is caused by an enlarged SR calcium concentration $[Ca^{2+}]_{sr}$. Originally, this was kept constant at $[Ca^{2+}]_{sr0}$ (1 mM) [Bers, 2002], but needed to be recalculated when isoproterenol was injected. For this, the new concentration $[Ca^{2+}]_{sr1}$ is calculated as a function of the ratio of influxes between a control and isoproterenol perfused

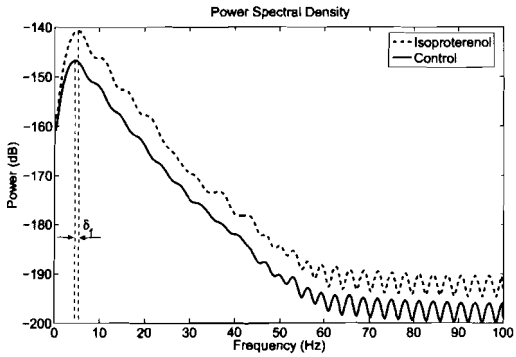

Figure 4: Frequency spectrum of control and isoproterenol heart. Difference in frequency is denoted by δ_f. The high peak is the dominant frequency that corresponds to the heartbeat.

myocardium (equation 18).

$$I_{in1} = g_l \cdot \frac{[Ca^{2+}]_{sr1} + [Ca^{2+}]_{ex0}}{2} \tag{17}$$

$$[Ca^{2+}]_{sr1} = ([Ca^{2+}]_{sr0} + [Ca^{2+}]_{ex0}) \cdot \frac{I_{in1}}{I_{in0}} - [Ca^{2+}]_{ex0} \tag{18}$$

The ratio $\frac{I_{in1}}{I_{in0}}$ is the relative increase of influx due to the perfusion of isoproterenol, and can be derived from estimates of the permeability g_l, which can be estimated very reliable, elucidated in section 5.

Experimental data

Experimental data was obtained from isolated intact Sprague-Dawley rat hearts. The hearts were studied in a Langendorff system. The intracellulair free calcium concentration $[Ca^{2+}]_i$ was determined with the Indo-1 fluorescence technique, and digitally stored with a sample frequency of 200 Hz [Ivanics, 2001]. For the isoproterenol perfused hearts, 5nM of isoproterenol was perfused to increase calcium concentration levels. All data was supplied by the Institute of Human Physiology of the Semmelweis University in Budapest (Hungary). Table 2 gives an overview of important data features of seven hearts, with their diastolic and systolic levels in control situation as well as isoproterenol situation and the dominant frequency (heartrate).

A peak detection algorithm was implemented to calculate the cycle times T and halftime t_h of the experimental data, and to determine the start of each heartbeat (to activate the modeled action potential). The found peaks were also visually checked, to see if any peaks were missed, or false peaks were returned. From an experimental dataset 25 calcium cycles were visually selected.

Initial values of the parameters were chosen as to be in the same range of earlier estimation results ([Riel, 2003], [Buijs, 2002]). To check if the algorithm converges to unwanted (local) minima, a large amount (N=250) of parameter estimates were obtained, with various initial values. Plots of these results can be seen in figure 17, 18 and 19 of appendix C. These plots show that there were no unwanted local minima, and the solution converged to one global minimum.

In total seven different datasets were used for evaluating the methods. Three of them were measurements done in 2002, and the remaining four were from 2005. The measurements of 2005 revealed some new dynamics. These dynamics were visible as a hump in the diastolic period [Ruijs, 2006]. The 2002 measurements did not reveal these dynamics. The three compartment model did not reckon with these dynamics, visible in the frequency range between 15 en 30 Hz. A low pass filter with a cut-off frequency of 15 Hz was used therefor to filter these unmodeled dynamics.

5 Results

Weighting vector

In section 2, a weighted objective cost function was introduced (equation 15). For the calcium handling case this becomes;

Table 2: Overview of 7 experimental datasets

	020920a	021015b	021016a	050914b	050920a	050921a	050922b
control							
$[Ca^{2+}]_{min}$ (mM)	141±4	104±5	173±6	175±6	126±8	168±9	135±7
$[Ca^{2+}]_{max}$ (mM)	335±9	234±8	355±10	423±11	344±10	441±11	444±10
f_{hr} (Hz)	4.88	4.79	4.88	5.08	4.49	4.88	4.59
isoproterenol							
$[Ca^{2+}]_{min}$ (mM)	419±26	380±29	343±19	280±9	344±11	324±12	294±11
$[Ca^{2+}]_{max}$ (mM)	1260±108	801±55	670±42	879±34	856±36	772±18	864±30
f_{hr} (Hz)	5.47	6.25	6.05	5.47	5.47	6.05	5.27

$$F_{tot}(\hat{\theta}) = w_1 F_1(\hat{\theta}) + w_2 F_2(\hat{\theta}) \qquad (19)$$

Here, F_1 is the cost function incorporating the experimental calcium concentration, and F_2 the cost function incorporating the a priori known efflux-ratio. The question arises how the different objectives have to be weighted to one another. This weighting is only relative, and in the two-dimensional case of the calcium handling $W = [w_1, w_2] = [w, 1]$ is the weighting vector. When w is too small ($w \rightarrow 0$), the optimization algorithm only uses the a priori information in the costfunction, and when w is too large ($w \rightarrow \infty$), the opposite occurs. To select a proper value for w experimentally, the cost functions of both objectives are calculated for optimization runs of a single experimental setup with different weighting vectors. Figure 5 shows a part of these (normalized) contributions as a function of weighting w. For small values of w it is obvious that the contribution of the cost function of the first objective to the total error is big and that of the second objective small. For large values of w it is exactly the other way around. The cost functions are normalized to values of the cost functions for a very small weighting value ($w \rightarrow 0$) and a very large weighting value ($w \rightarrow \infty$).

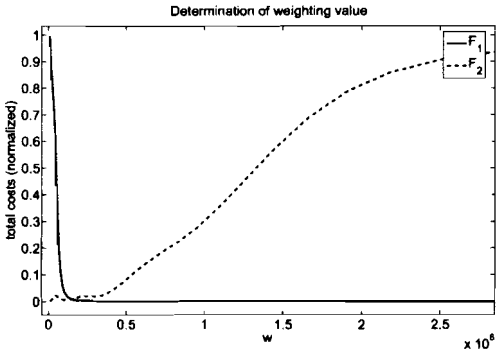

Figure 5: Normalized costs of first (solid) and second (dashed) objective of weighted objective optimization for various weighting values. The cost functions are normalized to values of the cost functions for $w \rightarrow 0$ and $w \rightarrow \infty$.

When these contributions are plotted as a function of each other, a plot that looks similar to the so-called pareto-front can be seen (figure 6). Calculating the pareto-front is a highly computing extensive method that is used in multi-objective optimization where no weighting vector is available. A pareto-front is a collection of points that are pareto-optimal. In other words, each of these pareto-optimal points can be seen as the best possible solution. It means that attempts of improving one objective will result in deterioration of the other. This study deals with a weighted objective optimization problem, and parallel to pareto-analysis, one point from the solution front is selected as the final solution. Here, this point is coupled to a certain weighting

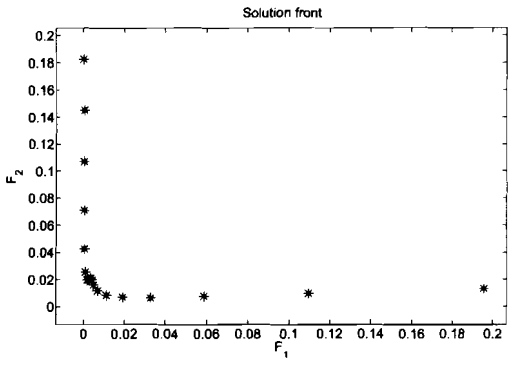

Figure 6: Solution front of weighted objective optimization. This plot has close resemblance with the pareto-front. Pareto is used to solve a multi-objective optimization problem without the use of weighting. Here, the points are generated by different weighting values, what makes it different than pareto.

value, which is the weighting w selected for the weighted costfunction.

Model-to-model identification

As a first step, a model-to-model identification approach was used, and two-dimensional contourplots of the cost functions of the separate objectives where drawn, as a function of the modelparameters. With these plots, it can easily be seen where the problem areas are for the identifiability. Figure 7 shows the first objective contourplots of V_m versus k_m (left), V_m versus g_l (middle) and V_m versus k_{ncx} (right). For the other combinations see appendix B. Figure 8 shows the same combinations, but now using only the a priori information in the cost function (the second objective). The true modelparameters θ_{true}, which are known in a model-to-model approach are indicated with a cross.

When the separate contourplots are combined as was discussed in the weighted objective optimization section (so optimizing with use of experimental data and a priori information), one can see the improvements in the identifiability of the model parameters (figure 9). Only the contour plot of SERCA parameters V_m and k_m forms an exception.

Parameter estimation

Control case

For seven intact rat control hearts the model-parameters were estimated. With use of the FIM a measure for the uncertainty was calculated as the relative standard deviation per parameter. Figure 10 shows the estimation results of one control heart (ID: 021016a) when no a priori information is used (only experimental data) in the cost function, as well as the weighted objective parameter estimation, thus with the a priori information and experimental data, and when only the a priori information is used in the cost function.

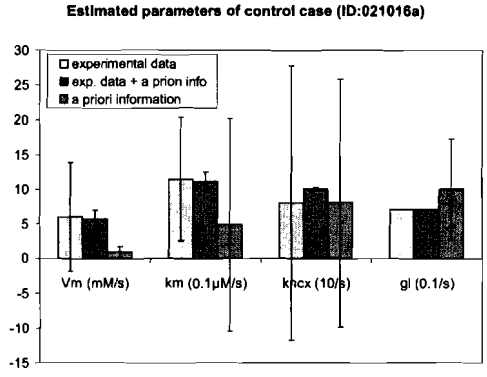

Figure 10: Estimates of the four model parameters for control case (ID:021016a).

The results show more or less a numerical representation of the model to model contourplots. It is obvious that k_{ncx} can be estimated with a much higher accuracy when experimental data and a priori information are incorporated in the cost function compared to the cost functions without. Without a priori information it can be seen from figure 7 (right plot), and also from figure 14 in appendix B (middle and right plot) that k_{ncx} can hardly be estimated, resulting in large deviations from the (unknown) true parameter.

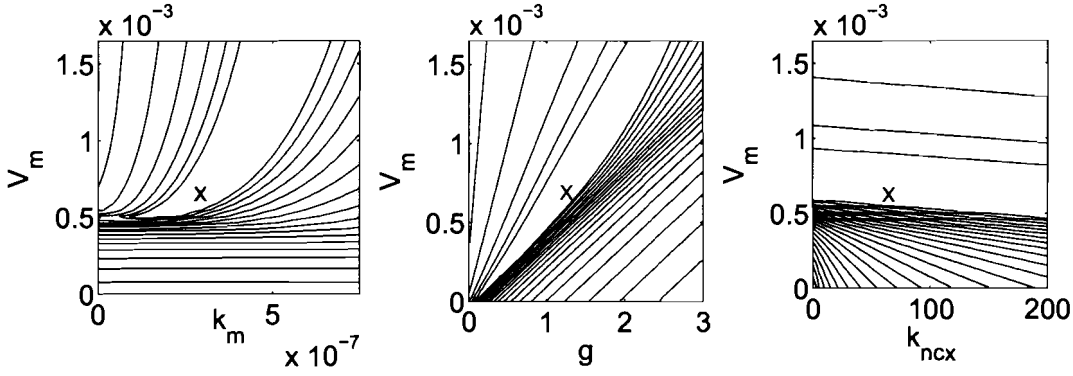

Figure 7: Two dimensional model-to-model contourplots of F_1. V_m vs. k_m (left), V_m vs. g_{lump} (middle), V_m vs. k_{ncx} (right). In model-to-model optimization the optimal minimum (for $\theta = \theta_{true}$) is known (indicated with a cross). It is obvious that this optimum is far from well defined.

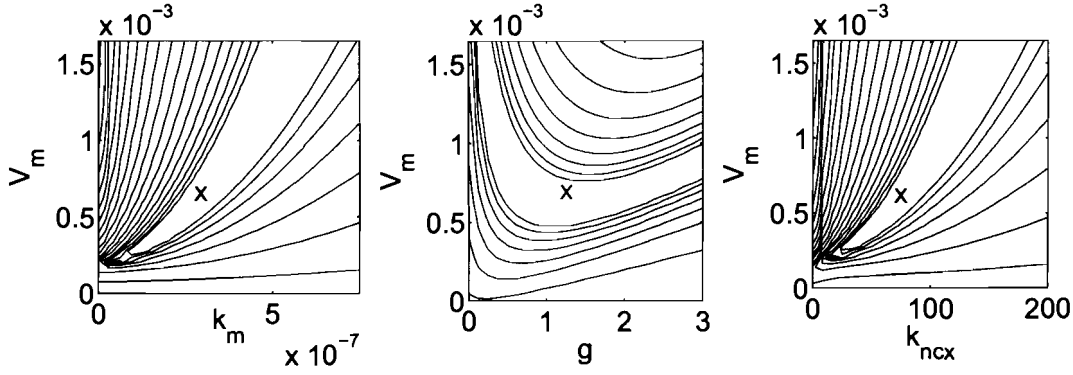

Figure 8: Two dimensional model-to-model contourplots of F_2. V_m vs. k_m (left), V_m vs. g_{lump} (middle), V_m vs. k_{ncx} (right). Also here the minimum (again indicated with a cross) is not well defined.

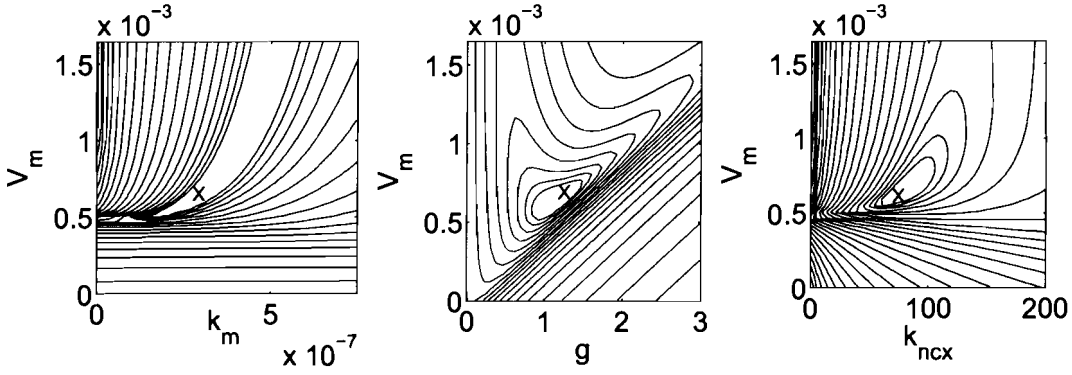

Figure 9: Two dimensional model-to-model contourplots of F_{tot}. V_m vs. k_m (left), V_m vs. g_{lump} (middle), V_m vs. k_{ncx} (right). Combining F_1 and F_2 in one weighted objective shows a much better defined minimum (defined with a cross) for the middle and right plot. The left plot (V_m vs. k_m) remains more or less bad unchanged.

The right plots of figures 7, 8 and 9 show the improvement of using a priori information by a change from a long stretched bathtub like minimum in figure 7 to a well defined convex minimum in figure 9. Another case is the lumped permeability g_l, which is already well defined (figure 7 (middle plot) and figure 14 (left and right)). So, even without a priori information, this parameter can be estimated with a high reliability. Only the experimental data is inevitable here. Without this data, large deviations can be seen for g_l.

The dependency between the two SERCA parameters V_m and k_m becomes clear in the left plot of figure 7. The contourplot of this parameter combination allows different sets of SERCA parameters that can be returned from the optimization algorithm, depending on initial values. The result of this are extremely high uncertainties, up to several hundreds percents of the estimated value. A contourplot of the a priori information concerning the SERCA parameters (left plot of figure 8) shows more or less the same behavior as the single-objective contourplot (figure 7). The minimal cost valley is somewhat narrower, which results in an increased estimation accuracy (see also figure 10). Still, there remains a higher uncertainty than, for example, the other two parameters (k_{ncx} and g_l) in the weighted objective optimization.

Numerical results of the parameter estimation of the normal (only experimental data) and weighted optimization of all control cases can be seen in table 3 and 4 in appendix D.

Isoproterenol case

The optimal experiment design section (section 4) already discussed the difficulties with the SERCA parameters. The model-to-model contourplots from the previous (figure 7, 8 and 9) underline this problem. The same long stretched 'bathtub' like valley of minima in contourplots of both objectives indicated a bad identifiability (the left plots of figure 7, 8 and 9), and although using the a priori information improved this identifiability, the uncertainty was still quite large.

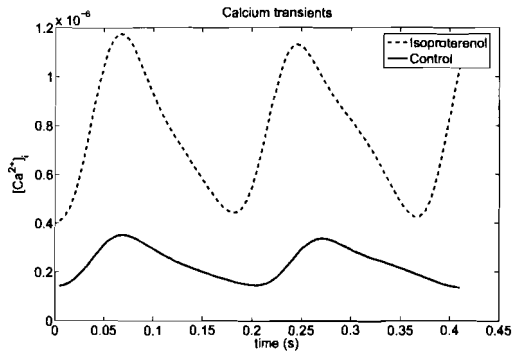

Figure 11: Calcium transients of control (solid) and isoproterenol infused heart (dashed). Differences can be seen in amplitude and end-diastolic and end-systolic calcium levels. Also the dominant frequency (heartbeat) differs a little bit.

By infusing isoproterenol in to the cytoplasm, the diastolic and systolic levels of the intracellular calcium concentration increases, covering a larger dynamical range of the SERCA kinetics (see section 4). Figure 11 shows the calcium transients in the cytoplasm for a control heart and a heart perfused with isoproterenol.

As was discussed in section 4, the SR calcium concentration $[Ca^{2+}]_{sr}$ for the isoproterenol case was recalculated. For the same control heart as used before (ID: 021016a) isoproterenol was infused and the new SR concentration $[Ca^{2+}]_{sr1}$ was calculated. For this case $[Ca^{2+}]_{sr1}$ was 2.05, which means an increase in the SR concentration of 105%.

It is assumed that isoproterenol only has effect on the working of SERCA, and therefor the SL/SR permeability g_l and Na^+/Ca^{2+} rate coefficient k_{ncx} are kept fixed. SERCA parameters V_m and k_m were re-estimated with g_l and k_{ncx} kept fixed. When isoproterenol was injected, no a priori information about the efflux-ratio is available anymore. Due

to isoproterenol the amount of calcium that flows through SERCA and NCX, and thus the ratio is not necessarily valid anymore. So parameter estimation must be done with single-objective optimization. Figure 12 shows the re-estimated SERCA parameters for the same heart as used before (ID: 021016a) where isoproterenol was perfused in the myocardium. An overview of all re-estimated SERCA parameters, as well as the new SR concentration can be found in Appendix E (table 5).

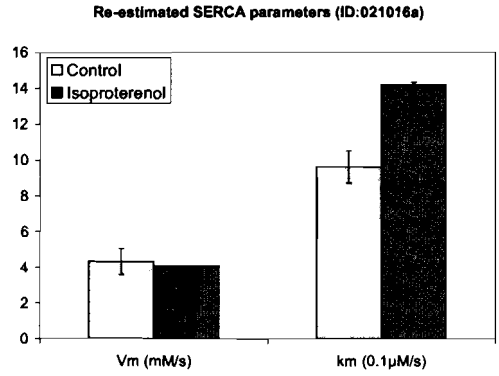

Figure 12: Re-estimated SERCA parameters of isoproterenol perfused heart (ID:021016a).

Compared to earlier estimates of the SERCA parameters, parameter estimations of the isoproterenol infused heart show a further increase of the reliability, measured by the standard deviation. The uncertainty can be graphically presented as was explained in section 2 with the eigenvalues en eigenvectors of the FIM (figure 13). The smaller uncertainty ellips of the isoproterenol infused heart shows that these SERCA estimates are more reliable than the control case estimates.

6 Discussion

Improving the reliability of the estimated model parameters was achieved by incorporating secondary information sources and taken into account in a weighted objective optimization. For the calcium handling case the method proved to be successful. It was hy-

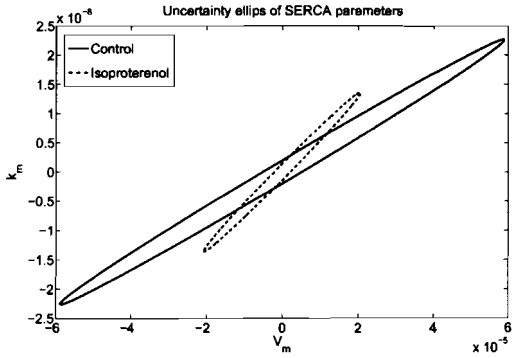

Figure 13: Uncertainty ellips of SERCA parameters of control (solid) and isoproterenol infused heart (dashed). Improvements in the reliability for isoproterenol can be seen in the smaller volume of this ellips.

pothesized that the quality of system identification improves when using additional information (if this a priori information is correct), and this article elaborates extensively how this could be achieved. Considering the case study as a typical example of a dynamic nonlinear system with sparse data, the results demonstrated the positive effect of the weighted objective optimization on the reliability of the parameter estimates.

When dealing with multi-objectives optimization, where several (conflicting) objectives have to be satisfied, several methods can be used [Sendin, 2005]. When no weighting factors are available to weigh the different objectives, as is done in this study, an optimal solution has to be selected from the pareto-front, which is the collection of pareto optimal points. Creating this pareto-front is a very time-consuming method. This study combines different objectives into one weighted objective, where the weighting vector is determined a priori. This value is determined experimentally based on a single dataset and used for all experiments of the calcium handling case study. Calculating this value for every experiment is very time consuming (just like calculating the pareto front), which makes this subjective approach more flexible. If any

information concerning this relative weighting is available, a more objective solution can be guaranteed.

Intuitively, a constrained optimization algorithm could be suggested for incorporating a priori information, where the a priori information restricts parameter solutions in the solution space. Caution has to be taken when using a constrained optimization for physiological applications. Obtaining a priori information from physiological systems results rarely in exact facts about system variables. It is more realistic to allow small deviations from the a priori information. Also the flux ratio presented in section 3 is based on estimates of the integrated fluxes through the various pumps [Bassani, 1994]. Bassani et al. already suggested recommendations to refine the estimates by better calibration of the fluorescence technique and a more thorough knowledge of the physiology of the pumps. Incorporating physiological information into a constrained optimization setting is therefor not recommended, because of these unknown deviations which is more difficult to take into account in constrained optimization.

Alternatively, a softer version of constrained optimization is an approach which uses penalty functions, that penalizes deviations from the quantitative measurements that are too big, allowing small deviations. Other studies already presented this way of incorporating a priori information in the system identification of physiological models. In [Riel, 2003], accounting a relative weighting to indicate the importance of the penalty, as well as the determination of the allowed deviations is determined rather arbitrary.

Other studies also use Bayes' theorem for incorporating any information based on the statistical information of parameters to support the experimental (a posteriori) data [Perttunen, 1989]. Bayesian approaches incorporate information about the a priori known distribution of the model parameters as quantative information [Sparacino, 2000], which is available for example from past research. Depending on the kind of a priori information that is available for system identification, the weighted objective optimization approach elucidated in this study or a Bayesian approach is preferable. A Bayesian method needs (statistical) information about the model parameters, whereas this study will do with information concerning variables of the system. A priori information directly concerning the model parameters is often more difficult to obtain, whereas a priori system information can more or less be information of any kind, which makes the weighted objective optimization a more generic approach.

Op den Buijs presented an overview of references with in vitro values of SERCA parameters in different situations (page 21 of [Buijs, 2002]). For isolated myocytes, similarities can be seen in the estimation of k_m between the overview of Op den Buijs and table 4, whereas V_m in the overview of Op den Buijs is much smaller. These deviations can be explained by the fact that the overview deals with isolated myocytes, instead of in vivo myocytes. With in vivo research, the behavior of the system within its environment is studied, which is favorable to discriminate between conditions of the system, for example concerning health. In vitro research lacks this environmental influence, which can be the cause for the difference between parameter values. So, the difficulty in obtaining reliable parameter estimates pays off in the profit of obtaining more clinical reliable values.

Perfusing the myocardium with isoproterenol resulted in the aimed for reliability improvements of the SERCA model parameters V_m and k_m. The physiological interpretation of changes in parameters values between the control and isoproterenol cases is less clear. It is believed that infusing isoproterenol result in an increased working of SERCA [Kaasik, 2001], visible by an increasing in both V_m and k_m. In all seven cases V_m gives a lower estimate for the isoproterenol

perfused cases, and k_m show various changes (both increasing and decreasing). At the moment there is no (physiological) explanation, and possibly a more physiological approach can describe this phenomenon.

In some of the measurements (as explained in section 4) a hump was detected in de down slope of the calcium transients. This hump was filtered out from the signal, because it was not taken into account in the model. The model of SERCA was not sufficient to describe this phenomenon, and without the low pass filter SERCA parameters drifted away to extreme (non-physical) values. This makes clear that the model needs adaption when this hump is taken into account. A more physiological description of the phenomenon can be found in [Jiang, 1998].

Isoproterenol was used in the experiment design to achieve increased calcium concentrations in the myocardium. Isoproterenol is a β-adrenergic stimulator, known for increasing contractility of the muscle fibers, caused by larger calcium transients. The results show an increased reliability of the estimated SERCA parameters when isoproterenol is used, compared to a normal control case. Other possibilities to increase calcium concentrations can be achieved by changes in input (input design). Changes in the frequency of the action potential (pacing) also resulted in changes in concentrations [Ruijs, 2006], but these changes where too small to have effect on the reliability of the SERCA parameters (results not shown). Therefor isoproterenol was favorable for the experiment design.

In system identification, validation is an important step to evaluate if the model describes the system well enough. For this, validation data is the data that is not used to build the model (estimation data). The problem of the systems described in this article, is the scarcity of the data. From one dataset (containing several hundreds of transients) only a small number of transients (25) are used as estimation data, but the remaining transients will do no good as validation data, as they contain the same dynamics as the estimation data. When the input can be changed, derivations on the data can be used for validation, but for obtaining in vivo measurements, not much can be changed in the input. Pacing was described earlier, and is a possibility for input design. Unfortunately, the effects are small, so validation remains very limited.

The aim of using minimal models like the one in this study is to classify different system conditions. The results already showed this classification by a large diversity of estimated model parameters. This diversity prevent the option to use data of the different myocardia for validation. It is obvious that finding descent validation techniques is very difficult, and deserves a closer look for further research.

7 Conclusion

The goal of this study was to investigate if and how the identifiability of dynamic nonlinear systems that suffer from sparse experimental data could be improved and model parameters could be estimated with higher accuracy. To do this, secondary information sources were obtained, from which a priori information was derived and incorporated in a weighted objective optimization, combining the sparse available experimental data and a priori information.

As a representative dynamic nonlinear example of systems that suffer from sparse datasets, a biomedical system was taken as a case study. A three compartment model of the calcium handling in rat myocardia was proposed, and with experimental data four model parameters were estimated. Without additional information only one parameter could be estimated accurately. For a better accuracy of the other three parameters, information about flux ratio between the three compartments was incorporated in the weighted objective optimization. It was

shown that the reliability of the parameter estimates was improved with weighted objective optimization. This improvement was measured as the standard deviation per model parameter.

This study provided several key improvements. At first, it can be mentioned that the weighted objective optimization proved to be an intuitive and flexible method to combine the sparse experimental data and a priori information in the minimization algorithm.

Furthermore, it appeared to be very advantageous that information concerning system variables could be used as quantitative a priori information, whereas a typical Bayesian approach needs parameter specific information.

Finally, a major advantage of the biomedical application in this study is the improvement to do reliable in vivo research. In biomedical research there is an increasing need to study how biological parameters change as a result of disease or therapy in the intact system. In vivo research is the favorable method when the aim is to discriminate between these system conditions. The drawback of doing in vivo research is the scarcity of data, which makes it more difficult to do reliable parameter estimations. This study shows that reliable estimates can be obtained, and thus in vivo research can be done more reliably, despite its drawbacks.

References

[Balke, 1994] Balke, C.W. et al.; Processes that remove calcium from the cytoplasm during excitation-contraction coupling. *J. Physiol. 474.3, 1994, pp. 447-462.*

[Bassani, 1994] Bassani, J.W.M. et al.; Relaxation in rabbit and rat cardiac cells: species-dependent differences in cellular mechanims. *J. Physiol. 476.2, 1994, pp. 279-293.*

[Bers, 2002] Bers, D.M.; Cardiac excitation-contraction coupling. *Nat. 415, January 10 2002, pp. 198-205.*

[Buijs, 2002] Buijs, op den, J.; Modeling of Calcium Dynamics in the Intact Rat Heart. *Practical training report, September 2001, 02/BMT/S02.*

[Buijs, 2005] Buijs, op den, J. et al.; β-Adrenergic activation reveals impaired cardiac calcium handling at early stage of diabetes. *Life Sciences 76, 2005, pp. 1083-1098.*

[Damen, 2003] Damen, A; Physiological Processes and Parameter Estimation. *July, 17, 2003.*

[Fabiato, 1983] Fabiota, A.; Calcium-induced release of calcium from the cardiac sarcoplasmic reticulum. *Am. J. Phys. 245 (Cell. Phys. 14), pp. C1-14.*

[Flaherty, 2005] Flaherty, P. et al.; Robust design of biological experiments. *Preproc. of the Neural Information Processing Symposium 2005, Vancouver, Canada, December 2005.*

[Hidalgo, 2000] Hidalgo, M.E. et al.; Numerical and Graphical Description of the Information Matrix in Calibration Experiments for State-Space Models. *Wat.Res. Vol.35, No.13, 2001, pp 3206-3214.*

[Hove-Madsen, 2001] Hove-Madsen, L. et al.; Characterization of the relationship between $Na^+ - Ca^{2+}$ exchange rate and cytosolic calcium in trout cardiac myocytes. *Eur. J. Physiol 441, 2001, pp. 701-708.*

[Ivanics, 2001] Ivanics T. et al.; Concomitant accumulation of intracellular free calcium and arachidonic acid in ischemic-repefused rat heart. *Mol. Cell. Biochem. 226, 2001, pp. 119-128.*

[Jiang, 1998] Jiang, Y. et al.; Basis for late rise in fura 2 R signal reporting $[Ca^{2+}]_i$ during relaxation in intact rat ventricular trabeculae. *Am. J. Physiol.; Cell Physiol. 274, 1998, pp C1273-C1282.*

[Kaasik, 2001] Kaasik, A. et al.; Decreased expression of phospholamban is not associated with lower β-adregenric activation in rat atria. *Mol. Cell. Biochem. 223, 2001, pp. 109-115.*

[Lin, 1976] Lin, J.G.; Multiple-Objective Problems: Pareto-Optimal Solutions by Method of Proper Equality Constraints. *IEEE trans. autom. contr. 5, October 1976, pp. 641-650.*

[Lytton, 1992] Lytton J. et al.; Functional Comparisons between Isoforms of the Sarcoplasmic or Endoplasmic Reticulum Family of Calcium Pumps. *J. Bio. Chem. 20, July 15 1992, pp. 14483-14489.*

[Ober, 2002] Ober, R.J. et al.; achievable accuracy of parameter estimation for multidimensional NMR experiments. *J. of magnetic resonance 157, July 2002, pp. 1-16.*

[Perttunen, 1989] Perttunen, C.D.; Bayesian model parameter estimation of systems subject to random input and output measurement error. *Proc. IEEE int. conf. on System Engineering, Fairborn, USA, August 1989, pp. 227-230.*

[Riel, 2003] Riel, van, N.A.W. et al.; System identification to analyse changed kinetics of SERCA in intact rat heart. *Proc. 5^{th} IFAC Conf. Mod. and control in biom. sys., Melbourne, Australia, August 2003, pp. 123-128.*

[Riel,2006] Riel, van, N.A.W. et al.; Parameter estimation in models combining signal transduction and metabolic pathways: The dependent input approach. *IEE Proc. Systems Biology, to be published.*

[Ruijs, 2006] Ruijs, L.S., et al.; Adaption of the intact rat heart to changes in workload. *Practical training report, February 2006, 06/08.*

[Sendin, 2005] Sendin, O.H., et al.; Model Based Optimization of Biochemical Systems Using Multiple Objectives: A Comparison of Several Solution Strategies. *Mathematical and Computer Modelling of Dynamical Systems, in press.*

[Sparacino, 2000] Sparacino, G. et al.; Maximum-Likelihood Versus Maximum a Posteriori Parameter Estimation of Physiological System Models; The C-peptide Impulse Response Case Study. *IEEE trans. bio. eng. 47, no. 6, june 2000, pp. 801-811.*

[Wagner, 1994] Wagner, J. et al.; Effects of rapid buffers on Ca^{2+} diffusion and Ca^{2+} oscillations. *Biophys. J. 67, July 1994, pp. 447-456.*

[Winslow, 1998] Winslow, R.L., et al.; Mechanisms of Altered Excitation-Contraction Coupling in Canine Tachycardia-Induced Heart Failure, II. Model studies. *Circ. Res. 84, 1999, pp. 571-586.*

A Derivation of cost function

If the residuals have a Normal distribution $\xi(k,\hat{\boldsymbol{\theta}}) \sim N(0,\sigma_\xi^2)$, and the samples are independently and identically distributed (i.i.d.), the probability density function $p(\boldsymbol{\xi}(\hat{\boldsymbol{\theta}}))$ is defined as

$$p(\boldsymbol{\xi}(\hat{\boldsymbol{\theta}})) = \prod_{k=1}^{K} p(\xi(k,\hat{\boldsymbol{\theta}})) = \left(\frac{1}{\sqrt{2\pi}\sigma_\xi}\right)^K \cdot e^{-\sum_{k=1}^{K}\frac{\xi(k,\hat{\boldsymbol{\theta}})^2}{2\sigma_\xi^2}} \tag{20}$$

This can also be written as the likelihood function $L(\boldsymbol{\xi}(\hat{\boldsymbol{\theta}}))$

$$L(\boldsymbol{\xi}(\hat{\boldsymbol{\theta}})) = \prod_{k=1}^{K} p(\xi(k,\hat{\boldsymbol{\theta}})) = \left(\frac{1}{\sqrt{2\pi}\sigma_\xi}\right)^K \cdot e^{-\sum_{k=1}^{K}\frac{\xi(k,\hat{\boldsymbol{\theta}})^2}{2\sigma_\xi^2}} \tag{21}$$

The likelihood function indicates the probability of occurrence of a measurement with a possible set of parameters $\boldsymbol{\theta}$. The maximum of this likelihood gives the eventually wanted estimation of the parameters $\hat{\boldsymbol{\theta}}$. This is called the Maximum Likelihood Estimator of $\boldsymbol{\theta}$.

The maximum of the likelihood function $L(\boldsymbol{\xi}(\hat{\boldsymbol{\theta}}))$ is equal to the minimum of $-\ln(L(\boldsymbol{\xi}(\hat{\boldsymbol{\theta}})))$. For that to be true the first derivative of $L(\boldsymbol{\xi}(\hat{\boldsymbol{\theta}}))$ and $-\ln(L(\boldsymbol{\xi}(\hat{\boldsymbol{\theta}})))$ both need to be zero, and their second derivative need to be respectively negative and positive. The first derivative of $-\ln(L(\boldsymbol{\xi}(\hat{\boldsymbol{\theta}})))$ is

$$\frac{\partial(-\ln(L))}{\partial\hat{\boldsymbol{\theta}}} = \frac{\partial(-\ln(L))}{\partial L}\frac{\partial L}{\partial\hat{\boldsymbol{\theta}}} = -\frac{1}{L}\frac{\partial L}{\partial\hat{\boldsymbol{\theta}}} \tag{22}$$

Where both L and $-\ln(L)$ has their extremum at zero. The second derivative of $-\ln(L(\boldsymbol{\xi}(\hat{\boldsymbol{\theta}})))$ can be written as

$$\frac{\partial^2(-\ln(L))}{\partial\hat{\boldsymbol{\theta}}^2} = \frac{\partial}{\partial\hat{\boldsymbol{\theta}}}\left(-\frac{1}{\partial L}\frac{\partial L}{\partial\hat{\boldsymbol{\theta}}}\right) = -\frac{1}{L}\frac{\partial^2 L}{\partial\hat{\boldsymbol{\theta}}^2} \tag{23}$$

Which proves that the second derivatives of L and $-\ln(L)$ have an opposite sign.

If the likelihood function $L(\boldsymbol{\xi}(\hat{\boldsymbol{\theta}}))$ is transformed into its negative natural logarithm version, the function becomes

$$-\ln(L(\boldsymbol{\xi}(\hat{\boldsymbol{\theta}}))) = \frac{1}{2\sigma_\xi^2}\sum_{k=1}^{K}\xi(k,\hat{\boldsymbol{\theta}})^2 + K\cdot\ln(\sigma_\xi) + \frac{K}{2}\ln(2\pi) \tag{24}$$

Because only the first part is dependent on the parameters $\hat{\boldsymbol{\theta}}$, this part is looked upon for further calculation. The final costfunction for the datafit $F(\hat{\boldsymbol{\theta}})$ is

$$F(\hat{\boldsymbol{\theta}}) = \frac{1}{2\sigma_\xi^2}\cdot\sum_{k=1}^{K}\xi(k,\hat{\boldsymbol{\theta}})^2 = \frac{1}{2\sigma_\xi^2}\cdot\sum_{k=1}^{K}(\hat{y}(k,\hat{\boldsymbol{\theta}}) - y(k,\boldsymbol{\theta}_{true}))^2 \tag{25}$$

Where this function needs to be minimized to estimate the parameters $\hat{\boldsymbol{\theta}}$ of the model

$$\hat{\boldsymbol{\theta}} = argmin\{F(\hat{\boldsymbol{\theta}})\} \tag{26}$$

B Contourplots: Model-to-model identification

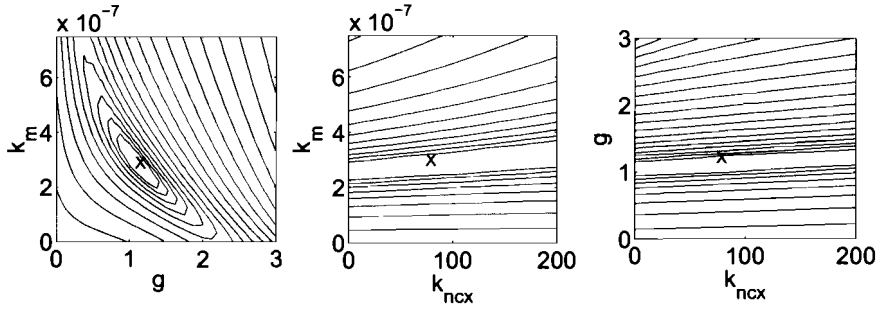

Figure 14: Two dimensional model-to-model contourplots of F_1. k_m vs. g (left), k_m vs. k_{ncx} (middle), g vs. k_{ncx} (right). The cross indicates the known true model parameterset $\boldsymbol{\theta}_{true}$.

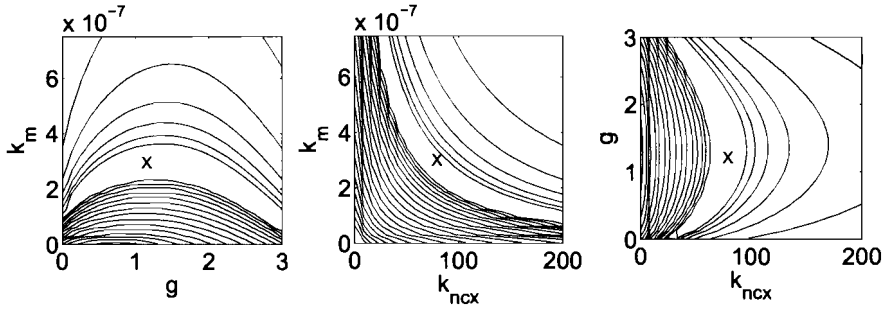

Figure 15: Two dimensional model-to-model contourplots of F_2. k_m vs. g (left), k_m vs. k_{ncx} (middle), g vs. k_{ncx} (right). The cross indicates the known true model parameterset $\boldsymbol{\theta}_{true}$.

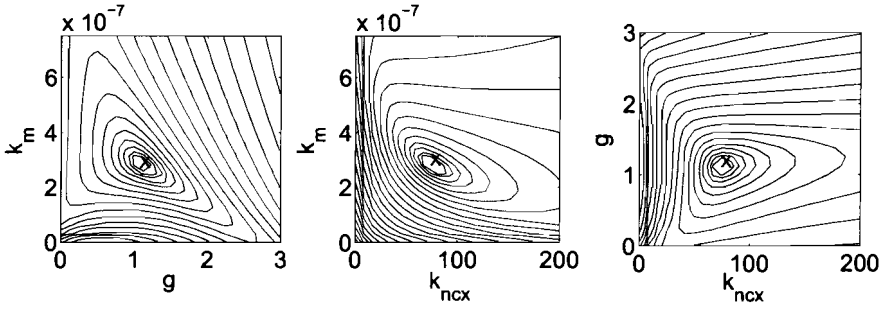

Figure 16: Two dimensional model-to-model contourplots of F_{tot}. k_m vs. g (left), k_m vs. k_{ncx} (middle), g vs. k_{ncx} (right). The cross indicates the known true model parameterset $\boldsymbol{\theta}_{true}$.

C Estimation results: Different initial values

Figure 17, 18 and 19 show the estimation results of two parameter combinations for various initial values of one case (ID:021016a). These initial values where chosen from a rather large range, randomly selected from a uniform distribution. The figures show once again the effect of incorporating a priori information into the minimization criterion. Furthermore, these figures show that their are no multiple (local) minima (in this range). So, their is no threat that the optimization algorithm will get stuck in a (local) minimum rather than the right (global) one.

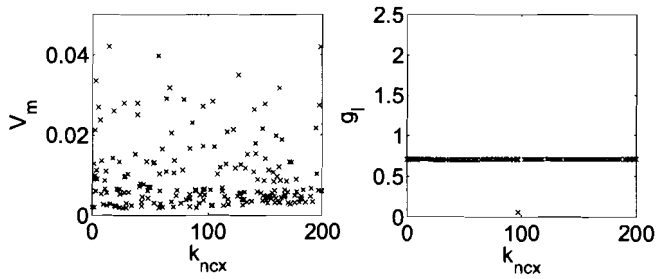

Figure 17: Estimation results of V_m versus k_{ncx} (left) and g_l versus k_{ncx} (right) for various initial values, taken from a uniform distribution, when only experimental data is used in the optimization algorithm.

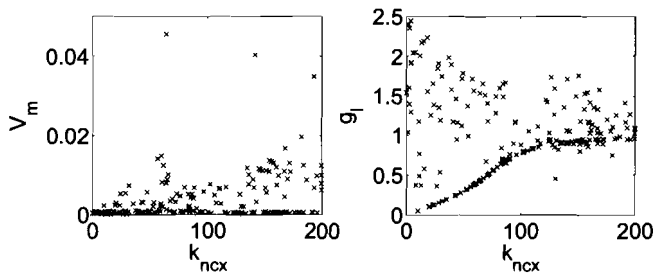

Figure 18: Estimation results of V_m versus k_{ncx} (left) and g_l versus k_{ncx} (right) for various initial values, taken from a uniform distribution, when only a priori information is used in the optimization algorithm.

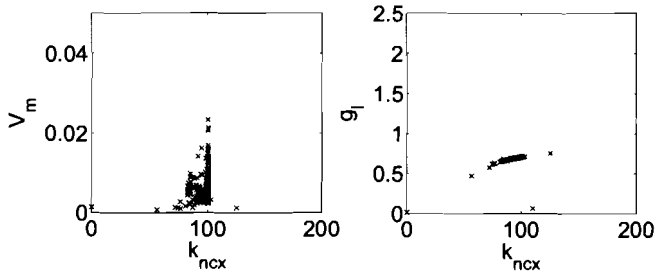

Figure 19: Estimation results of V_m versus k_{ncx} (left) and g_l versus k_{ncx} (right) for various initial values, taken from a uniform distribution, when both experimental data and a priori information are used in a weighted objective optimization.

D Estimation results: Single and multi objective optimization

Table 3: Parameter estimates of control hearts when using only experimental data in the cost function.

ID	Par.	value	unity	std(%)
020920a	V_m	2.04	mM/s	13.27
	k_m	0.53	μM	15.88
	k_{ncx}	80.11	$1/s$	233.30
	g_l	0.80	$1/s$	5.24
021015b	V_m	8.99	mM/s	174.45
	k_m	0.91	μM	97.08
	k_{ncx}	79.89	$1/s$	284.20
	g_l	0.66	$1/s$	0.93
021016a	V_m	6.02	mM/s	130.71
	k_m	1.14	μM	78.08
	k_{ncx}	79.99	$1/s$	246.86
	g_l	0.71	$1/s$	0.75
050914b	V_m	6.59	mM/s	62.49
	k_m	1.10	μM	39.53
	k_{ncx}	79.94	$1/s$	201.77
	g_l	1.00	$1/s$	0.71
050920a	V_m	11.31	mM/s	218.00
	k_m	1.42	μM	119.38
	k_{ncx}	79.98	$1/s$	219.49
	g_l	0.83	$1/s$	0.90
050921a	V_m	6.35	mM/s	50.27
	k_m	1.08	μM	32.62
	k_{ncx}	79.92	$1/s$	185.99
	g_l	1.09	$1/s$	0.71
050922b	V_m	3.21	mM/s	14.97
	k_m	0.72	μM	13.99
	k_{ncx}	80.01	$1/s$	169.60
	g_l	1.13	$1/s$	0.61

Table 4: Parameter estimates of control hearts when using a weighted objective optimization.

ID	Par.	value	unity	std(%)
020920a	V_m	2.09	mM/s	4.89
	k_m	0.55	μM	2.98
	k_{ncx}	117.81	$1/s$	0.79
	g_l	0.79	$1/s$	0.45
021015b	V_m	5.72	mM/s	118.96
	k_m	0.90	μM	61.71
	k_{ncx}	83.40	$1/s$	2.33
	g_l	0.44	$1/s$	1.74
021016a	V_m	5.67	mM/s	22.63
	k_m	1.11	μM	12.05
	k_{ncx}	101.10	$1/s$	1.09
	g_l	0.71	$1/s$	0.64
050914b	V_m	7.92	mM/s	18.45
	k_m	1.25	μM	9.82
	k_{ncx}	115.32	$1/s$	1.18
	g_l	0.99	$1/s$	0.63
050920a	V_m	5.99	mM/s	28.03
	k_m	1.05	μM	14.86
	k_{ncx}	98.06	$1/s$	1.33
	g_l	0.80	$1/s$	0.77
050921a	V_m	7.15	mM/s	14.92
	k_m	1.18	μM	8.03
	k_{ncx}	118.10	$1/s$	1.24
	g_l	1.07	$1/s$	0.62
050922b	V_m	3.24	mM/s	5.63
	k_m	0.74	μM	3.34
	k_{ncx}	119.78	$1/s$	1.19
	g_l	1.11	$1/s$	0.53

E Estimation results: Isoproterenol

Table 5: Re-estimated parameters of isoproterenol injected hearts, using only experimental data in the cost function.

ID	$[Ca^{2+}]_{sr1}$ (mM)	Par.	value	unity	std(%)
020920a	3.15	V_m	1.42	mM/s	2.46
		k_m	0.88	μM	2.59
021015b	3.08	V_m	2.04	mM/s	5.09
		k_m	0.86	μM	3.92
021016a	2.05	V_m	4.08	mM/s	1.74
		k_m	1.42	μM	1.00
050914b	2.63	V_m	2.46	mM/s	2.01
		k_m	0.84	μM	1.62
050920a	2.35	V_m	1.74	mM/s	2.39
		k_m	0.85	μM	1.93
050921a	1.55	V_m	3.22	mM/s	4.68
		k_m	1.15	μM	3.01
050922b	1.70	V_m	2.87	mM/s	3.21
		k_m	1.09	μM	2.20

F Matlab code

COST_CALCIUM

```
%Estimates model parameters and reliability
function [theta,ts_meas,cin_meas,cin_mod,FIM,std_theta,RESIDUAL,...
,Jacobian] = cost_calcium(theta_init,theta_fixed,position,obj_count,W,data_id,bnr)

global fs;

data=grab_data(data_id);
[T,dc,ts_meas,cin_meas,r_true,cin0,index_min,index_max] = data_calcium(data,bnr);

u = siginput2(T,dc);

options_lsq = optimset( 'Display',              'final',...
                        'MaxFunEvals',          400,...
                        'TolFun',               1e-3,...
                        'TolX',                 1e-8,...
                        'LargeScale',           'on');  %Trust region

lb = zeros(size(theta_init));
ub = [];

[theta,resnorm,RESIDUAL,EXITFLAG,OUTPUT,LAMBDA,Jacobian] = ,...
lsqnonlin('mod_calcium',theta_init,lb,ub,options_lsq,theta_fixed,position,...
,u,ts_meas,cin_meas,cin0,r_true,obj_count,W,index_min,index_max);

%covariance is inverse of Fisher Information Matrix
FIM = Jacobian'*Jacobian/var(RESIDUAL);
covar = inv(FIM);
std_theta = sqrt(diag(covar));

%%%%%%%%%%%%%%%%%%%%%%%%%%%%%%%%%%%%%%%%%%%%%%%%%%%%%%%%%%%%%%%%%%%%%%%%%%%%%%%
```

DATA_CALCIUM

```
%pre-processor for experimental data
function [T,dc,ts_meas,cin_meas,r_true,cin0,index_min,index_max,dc_per] = ,...
 data_calcium(data,bnr)

Ts = 1/fs;      %sample period [s]
cfreq = 15;     %cut-off frequency for lowpass filter [Hz]

%filter data with lowpass filter
B = fir1(20, cfreq/(fs/2));         %filter coefficients
cin_meas_raw = filtfilt(B, 1, data);
cin_meas_raw = 1e-9 * cin_meas_raw;          %from M to nM
```

```
%find local maxima/minima of calciumconcentration at end of systole/diastole
[index_min_raw,index_max_raw] = extrema(cin_meas_raw);

cin0=mean(cin_meas_raw(index_min_raw(bnr(1):bnr(2))));

%select data with chosen timespan
cin_meas = cin_meas_raw(index_min_raw(bnr(1))+1 : index_min_raw(bnr(2)));

%select timevector
ts_meas = (1:length(cin_meas))./ fs;
ts_meas = ts_meas';
T = diff(index_min_raw(bnr(1):bnr(2)));

%a priori VNCX/VSERCA ratio
r_true = 92/8;

%DETERMINING DUTYCYCLE
[dc,dc_per] = dutycin(cin_meas_raw,index_min_raw(bnr(1):bnr(2)));

[index_min,index_max] = extrema(cin_meas);

%%%%%%%%%%%%%%%%%%%%%%%%%%%%%%%%%%%%%%%%%%%%%%%%%%%%%%%%%%%%%%%%%%%%%%%%%%%%%%%
```

SIGINPUT2

```
%model for action potential (input)
function u = siginput2(T,dc_rel)

for k=1:length(T)
    dc(k) = dc_rel;
    tlin = (1:T(k))/fs;
    t_per = mod(tlin,T(k)+1);
    th_up = 0.01;
    u(sum(T(1:k))-T(k)+1:sum(T(1:k))) =,...
     (t_per.^4./(t_per.^4 + th_up.^4)).*(1 - t_per.^4./(t_per.^4 + dc(k).^4));
end
u = u/max(u);   %amplitude of inputfunction is 1

%%%%%%%%%%%%%%%%%%%%%%%%%%%%%%%%%%%%%%%%%%%%%%%%%%%%%%%%%%%%%%%%%%%%%%%%%%%%%%%
```

MOD_CALCIUM

```
%calculates error, used for LSQNONLIN
function [e,d1,d2,cin_mod] = mod_calcium(theta_var, theta_fixed, position,...
, u, ts_meas, cin_meas,cin0, r_true,obj_count, W,index_min,index_max)
```

```
theta_pos = set_par(theta_var, theta_fixed, position);

%Modeling of calcium transients, used for least squares methods (LSQNONLIN)
%use ODE23 solver (variable step)
OPTIONS = odeset('maxstep',1e-3);  %define maximal stepsize
[ts_mod,cin_mod]=ode23(@ode_calcium,ts_meas, cin0, OPTIONS, theta_pos, u);

[r_mod,int_VNCX_dias,int_VSERCA_dias] = obj_calcium2(theta_pos, cin_mod,...
, index_min, index_max);

w = W;
d1 = 1e9*(cin_mod-cin_meas)';
d2 = (r_mod-r_true);
e1 = w(1) * d1;
e2 = w(2) * d2;

if obj_count == 1
    e = e1;
elseif obj_count == 12
    e = [e1 e2];
elseif obj_count == 2
    e = e2;
end

%%%%%%%%%%%%%%%%%%%%%%%%%%%%%%%%%%%%%%%%%%%%%%%%%%%%%%%%%%%%%%%%%%%%%%%%%%%%%%%
```

EXTREMA

```
%determines minima and maxima
function [index_min,index_max] = extrema(data)

%remove trend from data
bp=[];
ii=1;
%select breakpoints to calculate trends
for i=1:length(data)
    if(mod(i,80)==0)
        bp(ii)=i;
        ii=ii+1;
    end
end
data = detrend(data,'linear',bp);

%small extra filter to filter out local extrema
for k=3:length(data)-2
    data(k) = data(k-1)+(data(k+1)-data(k-1))/2;
end
```

```
s = 10;
res = floor(length(data)/s);
for k=1:s
    max_est(k)=max(data(res*(k-1)+1:res*(k)));
    min_est(k)=min(data(res*(k-1)+1:res*(k)));
end

%Introduce upper and lower threshold to selects peaks
thres = mean(data)-0.3*(mean(data)-mean(min_est));   %-0.5*
thres2 = mean(data)+0.3*(mean(max_est)-mean(data));  %+0.5*

index_min = [];
index_min2 = [];
imin = 1;
index_max = [];
index_max2 = [];
imax = 1;
iprev_min = 1;
iprev_max = -15;

%check first 2 datapoints for minima/maxima
if ((data(1)<thres)&&(data(1)<data(2))&&(data(1)<data(3)))
    index_min(1) = 1;
elseif ((data(2)<thres)&&(data(1)>data(2))&&(data(2)<data(3)))
    index_min(1) = 2;
elseif ((data(1)>thres2)&&(data(1)>data(2))&&(data(1)>data(3)))
    index_max(1) = 1;
elseif ((data(2)>thres2)&&(data(1)<data(2))&&(data(1)>data(3)))
    index_max(1) = 2;
end

%check remaining points (except last 3) for minima/maxima
ld = length(data);

for i = 3:ld-3
    %find minima
    if ((data(i)<thres)&&(data(i-1)<data(i-2))&&(data(i)<data(i-1)),...
       &&(data(i)<data(i+1))&&(data(i+1)<data(i+2))&&(data(i+2)<data(i+3)))

        %if two minima are two close to each other, the right one has to be selected
        if i-iprev_min < (fs/12)
            %index_min(length(index_min)) = i;
            [temp,itemp] = min([data(iprev_min) data(i)]);
            index_min(imin) = iprev_min + (itemp-1)*(i-iprev_min);
        else
            index_min = [index_min; i]; %add new detected minimum to index
```

```
        end
        imin = length(index_min);
        iprev_min = i;

    %find maxima
    elseif ((data(i)>thres2)&&(data(i-1)>data(i-2))&&(data(i)>data(i-1)),...
            &&(data(i)>data(i+1))&&(data(i+1)>data(i+2))&&(data(i+2)>data(i+3)))
        %the latest detected minimum should replace previous
        if i-iprev_max < (fs/12)
            %index_min(length(index_min)) = i;
            [temp,itemp] = max([data(iprev_max) data(i)]);
            index_max(imax) = iprev_max + (itemp-1)*(i-iprev_max);
        else
            index_max = [index_max; i]; %add new detected minimum to index
        end
        imax = length(index_max);
        iprev_max = i;
    end
end

%check last 3 datapoints for minima/maxima
if((data(ld)<thres)&&(data(ld)<data(ld-1))&&(data(ld)<data(ld-2)))
    index_min = [index_min; ld];
elseif((data(ld-1)<thres)&&(data(ld-1)<data(ld-2))&&(data(ld-1)<data(ld)))
    index_min = [index_min; ld-1];
elseif((data(ld-2)<thres)&&(data(ld-2)<data(ld-1))&&(data(ld-2)<data(ld)))
    index_min = [index_min; ld-2];
elseif((data(ld)>thres2)&&(data(ld)>data(ld-1))&&(data(ld)>data(ld-2)))
    index_max = [index_max; ld];
elseif((data(ld-1)>thres2)&&(data(ld-1)>data(ld-2))&&(data(ld-1)>data(ld)))
    index_max = [index_max; ld-1];
elseif(((data(ld-2)>thres2)&&(data(ld-2)>data(ld-1))&&(data(ld-2)>data(ld))))
    index_max = [index_max; ld-2];
end

%%%%%%%%%%%%%%%%%%%%%%%%%%%%%%%%%%%%%%%%%%%%%%%%%%%%%%%%%%%%%%%%%%%%%%%%%%%%%%%
```

DUTYCIN

```
%calculates halftime for Sigmoid input function
function [dc,dc_per] = dutycin(cin_raw,index_min)

%cut data in single heartbeats
for k=1:length(index_min)-1

    data = cin_raw(index_min(k):index_min(k+1));
    data_dot = diff(data);
```

```
    %searched for point half of maximal influx
    [data_dot_max,i_max] = max(data_dot);
    dhalf = .5 * data_dot_max;

    %interpolation to find dutycycle
    for kk=i_max:length(data_dot)-1
        if((data_dot(kk)>data_dot(kk+1)) && (data_dot(kk)> dhalf),...
             && (data_dot(kk+1)< dhalf))
            kk_star = kk + (data_dot(kk) - dhalf)/(data_dot(kk)-data_dot(kk+1));
        end
    end
    dc(k) = 1.25 * kk_star/fs;
    dc_per(k) = 1.25 * (100 * kk_star ./(index_min(k+1)-index_min(k)));
end
dc = mean(dc);

%%%%%%%%%%%%%%%%%%%%%%%%%%%%%%%%%%%%%%%%%%%%%%%%%%%%%%%%%%%%%%%%%%%%%%%%%%%%%%%
```

SET_PAR

```
%set_par puts the fixed parameters and the parameters to be estimated in
%the right order.
function par_pos=set_par(par_var, par_fixed, position)

if nargin < 2
    par_fixed = [];
    position = [1 2 3 4];
elseif nargin < 3
    position = [1 2 3 4];
end

par_temp = [par_var par_fixed];

if length(par_temp) ~= length(position)
    error('number of parameters doesnt match');
end

for k=1:(length(par_var)+length(par_fixed))
    par_pos(position(k)) = par_temp(k);
end

%%%%%%%%%%%%%%%%%%%%%%%%%%%%%%%%%%%%%%%%%%%%%%%%%%%%%%%%%%%%%%%%%%%%%%%%%%%%%%%
```

OBJ_CALCIUM2

```
%determines experimental flux ratio
function [r_mod,int_VNCX_dias,int_VSERCA_dias] =,...
```

```
 obj_calcium2(theta, cin_mod, index_min, index_max)

Vmaxserca = theta(1);
Kmserca   = theta(2);
kncx      = theta(4);

int_VNCX_dias = [];
int_VSERCA_dias = [];

nmin = length(index_min);
nmax = length(index_max);

VNCX   = kncx .* cin_mod;
VSERCA = Vmaxserca * (cin_mod.^ns ./(cin_mod.^ns + Kmserca.^ns));

%diastole
for k=1:min(nmin,nmax)-1
    if(index_min(k) < index_max(k) && index_max(k) < index_min(k+1))
        int_VNCX_dias(k) = sum(VNCX(index_max(k):index_min(k+1)));
        int_VSERCA_dias(k) = sum(VSERCA(index_max(k):index_min(k+1)));
    elseif(index_max(k) < index_min(k) && index_min(k) < index_max(k+1))
        int_VNCX_dias(k) = sum(VNCX(index_max(k):index_min(k)));
        int_VSERCA_dias(k) = sum(VSERCA(index_max(k):index_min(k)));
    end
end

%wanted ratio of Vserca and Vncx is 92/8
r_mod = int_VSERCA_dias./int_VNCX_dias;

%%%%%%%%%%%%%%%%%%%%%%%%%%%%%%%%%%%%%%%%%%%%%%%%%%%%%%%%%%%%%%%%%%%%%%%%%%%%%%%
```

ODE_CALCIUM

```
%differential equation for model
function cin_dot = ode_calcium(t,cin,theta,u)

cin_dot=0;

Vmaxserca = theta(1);
Kmserca   = theta(2);
glump     = theta(3);
kncx      = theta(4);

%DHPR, RyR
cex0 = 1.5e-3;      %extracellular calcium concentration
csr0 = 1e-3;        %SR calcium concentration
```

```
%Buffersystems
Kd = [0.51e-6 0.87e-6 0.38e-6 87e-6];
B =  [70e-6 47e-6 24e-6 1124e-6];

u = u(floor(t*fs));

G = glump * (mean([cex0 csr0])) * u;        %because cex0 >> cin and csr0 >> cin

%Pump flows
VNCX   = kncx .* cin;
VSERCA = Vmaxserca * (cin.^ns /(cin.^ns + Kmserca.^ns));

%Calciumbuffers
for k=1:4
    CaBi(k) = B(k) .* Kd(k)./(Kd(k) + cin).^2;
end
CaB = 1 + sum(CaBi);

cin_dot = (-VNCX - VSERCA + G)/CaB;

%%%%%%%%%%%%%%%%%%%%%%%%%%%%%%%%%%%%%%%%%%%%%%%%%%%%%%%%%%%%%%%%%%%%%%%%%%%%%%%
```